Spectral analysis and second-order cyclostationary analysis of the non-stationary stochastic motion of a boring bar on a lathe

Y. Calleecharan

***Abstract*—In turning and boring, vibration is a frequent problem. The motion of a boring bar is frequently influenced by force modulation, i.e. the dynamic motion of the workpiece related to the residual rotor mass imbalance influences the motion of the motion of the boring bar via the relative dynamic motion between the cutting tool and the workpiece. Second-order cyclostationary analysis of the non-stationary stochastic motion of a boring on a lathe is carried out and compared with the conventional spectrum estimation method of the power spectral density. It is observed that the periodic nature of this dynamic motion suits well in the cyclostationary framework because of the rotating motion on the lathe. Also, it is found that cyclostationary analysis contains the time information in the metal cutting process and it can provide insight on the modulation structure of the frequencies involved in the boring operation.**

Index Terms—**boring bar, cyclostationary, lathe, power spectral density, second-order statistics**

NOMENCLATURE

α	cyclic frequency [Hz]
ε_r	normalised random error
τ	continuous time lag parameter [s]
a	cutting depth [mm]
CAF	cyclic autocorrelation function
CDD	cutting depth direction
CSD	cutting speed direction
DCS	degree of cyclostationarity
f	spectral frequency [Hz]
F_s	sampling frequency [Hz]
i	integer index
I	power spectral density estimate
L	data length
m	discrete time index
n	discrete time index
N	positive integer number
PSD	power spectral density
$\hat{r}$	CAF or autocorrelation estimate
SCDF	spectral correlation density function
s	primary feed rate [mm/rev]
$\hat{S}$	SCDF estimate
t	continuous time parameter [s]
T	continuous domain time period [s]
U	window-dependent bandwidth normalisation factor
v	cutting speed [m/min]
w	time window

subscripts & superscripts

k	integer index
p	integer index
s	sampling

Y. Calleecharan is with the Department of Mechanical and Production Engineering, University of Mauritius, Réduit, 80837, Mauritius (email: y.calleecharan@uom.ac.mu).

I. INTRODUCTION

THE presence of vibrations in the turning and boring operations in a lathe is a very common problem and leads to well-known undesirable effects such as degradation in the surface finish of the machined part, structural fatigue of the cutting tool and holder, and annoyingly high sound levels. Poor choices of cutting parameters, cutting of very hard materials, etc., typically lead to vibration problems. Tool chatter is an issue that has been studied in literature for a long time [1]. With the increasing demands of higher productivity coupled by the requirements for smaller tolerances in the machined part surfaces, the need arises to understand the dynamics in the cutting operation. Pioneering works in this field [2], [3] have been carried out in which the nature, causes and implications of the vibrations were unveiled and traditional spectral analysis techniques were used.

The dynamic motion of the boring bar in the metal cutting process originates from the deformation operation of the work material. This motion of a boring bar is frequently influenced by e.g. force modulation, i.e. the dynamic motion of the workpiece related to residual rotor mass imbalance influences the motion of the boring bar via the relative dynamic motion between the cutting tool and the workpiece. Now, if boring bar vibration is affected by force modulation, the vibration responses generally have non-stationary stochastic properties. However, there are strong indications due to the periodicity involved from the rotary motion on the lathe that the second-order statistic properties of the boring bar vibration have cyclostationary properties.

A number of experimental and analytical studies have been carried out on the study of tool vibration in turning. Most research has been carried out on the dynamic modelling of cutting dynamics [4]–[13] and usually concentrates on the prediction of stability limits as well as experimental methods for the estimation of model parameters related to the structural dynamic properties of the machine tool, the workpiece material, etc. A subset of the research on cutting dynamics has focussed on boring dynamics [14]–[19], which is more relevant to the present work. However, there are relatively few works which address the identification of dynamic properties of machine tool vibration [20]–[25] and especially the identification of dynamic properties of boring bar vibration [23]–[25]. In-depth literature surveys concerning the experimental and analytical studies are given in References [24], [25].

Vibration signals are usually investigated using signal processing tools. Usually, quantities such as variance, autocorrelation, power spectral density (PSD) and power spectrum are estimated for a vibration signal. Traditional time averaging or synchronous averaging are generally included in the estimation methods defined for the quantities mentioned previously. Care should be taken nevertheless with these stationary time-frequency methods since they can lead to ambiguous, if not misleading, results in an industrial environment where there is interference caused by random or periodic noise in the vicinity of the frequency bandwidth of interest. Synchronous averaging attenuates information in the vibration signal that is not harmonically related to the rotation. The part of the vibration signal related to the rotation may be investigated by e.g. the power spectrum estimator or by the PSD. More sophisticated and less common tools such as short time Fourier Transform, the pseudo Wigner-Ville Transform or the discrete

wavelet Transform include the time dimension parameter in the time-frequency analysis, but these methods have a severe drawback in that they cannot exploit any information which does not appear in the synchronous average such as periodically correlated random pulses or amplitude modulation of asynchronous signals which is common from rotating machinery [26].

In the case of periodically correlated random pulses or amplitude modulation of asynchronous signals that is common from rotating machinery, the second-order cyclostationary analysis method e.g. with its cyclic spectrum has proved to be useful—it is able to isolate amplitude modulation phenomena by its unique attribute of spectral correlation in the bi-frequency plane [26]. This paper uses both the traditional spectral analysis method namely the PSD and the less common second-order cyclostationary analysis on time vibration signals from the boring bar operation on a lathe to analyse the second-order characteristics of the boring process.

Though cyclostationary analysis was first applied in the field of telecommunications [27], several works [26], [28]–[31] have shown the usefulness of this technique in analysis and in condition monitoring of mechanical engineering equipment where rotating components exist. Cyclostationary analysis enables periodic amplitude modulation phenomena to distinguish themselves from other interfering vibrations or sounds on the shop floor and this allows in the case of amplitude-modulation signals to resolve the various components present in the signal. The usefulness of cyclostationary analysis is that firstly it is a tool that allows periodic phenomena to be distinguished from non-periodic ones as shown in Reference [32] and secondly, different periodic frequencies e.g. from rotating machines produce distinct frequency patterns in the bi-frequency plane from the cyclostationary analysis method [33]. It is the purpose of this article hence to demonstrate that the cyclostationary analysis framework is indeed a very suitable tool to investigate the force modulation phenomenon affecting the motion of the boring bar.

II. Experimental set-up

As with all machining operations, metal cutting takes place between a cutting tool and a workpiece material. For a lathe, the cutting tool is most often single-point attached to the tool holder e.g. a boring bar. The desired surface is created by providing suitable relative motion between the cutting tool and the workpiece material. This relative motion is composed of basically two components: primary- and secondary-feed motions. More specifically, the primary motion is generated by rotation of the workpiece material, while the secondary motion is the feed motion associated with the cutting tool. It is the simultaneous combination of these two relative motion components that lead to continuous chip removal from the workpiece material. The cutting operations have been carried out in a Mazak SUPER QUICK TURN—250M CNC turning center shown in Fig. 1 with 18.5 kW spindle power, maximal machining diameter 300 mm and 1007 mm between the centres. In order to save material, the cutting operation was performed as external turning operation, although a boring bar, WIDAX S40T PDUNR15, was used.

A. Measuring equipment and setup

In the vibration measurements, two PCB U353B11 accelerometers and a TEAC RD-200T DAT-recorder were used. The two accelerometers were mounted on the boring bar using threaded studs and they were placed as close as possible to the cutting tool bit—one in the cutting speed direction (CSD) and one in the cutting depth direction (CDD)—see Fig. 2.

Fig. 1. Figure shows the CNC equipment Mazak SUPER QUICK TURN used in the experiments

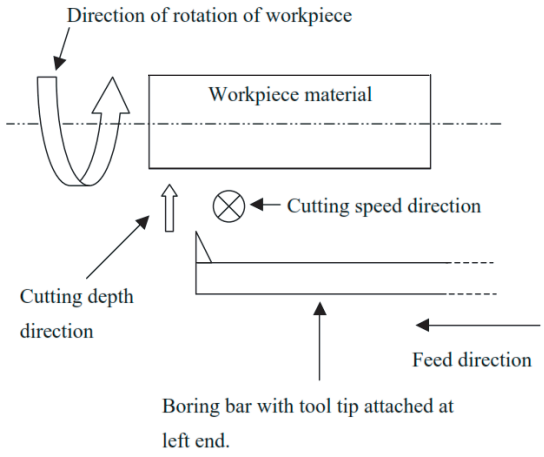

(a) Schematic plan view of experimental arrangement

(b) Experimental vibration measurement setup

Fig. 2. Top diagram illustrates a schematic plan view of boring bar arrangement with respect to the workpiece material. The cutting speed direction and the cutting depth direction are defined. Bottom diagram shows the two accelerometers mounted on the boring bar in the cutting speed direction and in the cutting depth direction respectively

B. Workpiece materials

Work materials are usually classified according to three production engineering application classes: K (cast irons), M (stainless steels) and P (alloyed steels), all standardised by ISO [34]. In the cutting experiments, three different workpiece materials, each belonging to a different class, have been used, namely: SS 0727-02 or nodular graphite cast iron as a K material, SS 2343-02 or austenitic stainless steel as an M material and SS 2541-03 or chromium molybdenum nickel steel as a P material. These materials have different properties from a production point of view. In American standards, the classes K, M and P correspond to AISI 80-55-06, AISI 316 and AISI 4340 respectively. The machinability or more specifically the cuttability of the materials differs and the chemical composition of the three materials, which is shown in Table I, is also different. The diameter of the workpiece materials is chosen large (around 200 mm); thus the workpiece vibrations may be neglected. Since the statistical properties of the cutting forces are to be investigated, the influence of the workpiece material is vital. The chemical composition and micro-structure of the materials as well as the strength and the thermo-dynamical properties determine the behaviour of the cutting process. The optimal workpiece material should, from a production engineering point of view, induce small cutting forces, be capable of producing a proper surface finish, have a fair chip breaking property, and not deteriorate the cutting tool. The selected materials have different properties with respect to these four aspects [21].

TABLE I
Chemical composition of workpiece materials

Production engineering application class	C [%]	Si [%]	Mn [%]	Cr [%]	Ni [%]	Mo [%]
K	3.7	2.2	0.4	Nil	Nil	Nil
M	0.05	Nil	Nil	18	12	2.7
P	0.36	0.27	0.62	1.53	1.41	0.17

C. Choice of cutting parameters

In the cutting experiments, standard 55° diagonal inserts have been used. They have tool geometry with the ISO code DNMG 150608-SL with chip breaker geometry for medium roughing. Different carbide grades but with the same geometries have been used for different materials. Carbide grade TN7015 was used for the cast iron and the alloyed steel materials, and carbide grade TN8025 was used for the stainless steel material.

The selection of the cutting data parameter space must be based on thorough knowledge of the cutting process itself. Excessive wear, catastrophic failure or plastic deformation may result if too high cutting speeds or feed rates are selected. This can in turn lead to results which are not characteristic to a turning operation under normal circumstances. The cutting data were chosen according to Table II. Also, no cutting fluid was applied during machining. The aim was to find a parameter space equal for all materials. However, it was found to be impossible to exceed 200 m/min in cutting speed for the stainless steel SS 2343-02.

TABLE II
Cutting parameter space for the three materials used in the experiments

Material	Parameter	Range
SS 0727-02	Feed, s [mm/rev]	0.1–0.3, step 0.1
	Depth of cut, a [mm]	2
	Cutting speed [m/min]	50–300, step 25
SS 2343-02	Feed, s [mm/rev]	0.1–0.3, step 0.1
	Depth of cut, a [mm]	2
	Cutting speed [m/min]	50–200, step 25
SS 2541-03	Feed, s [mm/rev]	0.1–0.3, step 0.1
	Depth of cut, a [mm]	2
	Cutting speed [m/min]	50–300, step 25

III. Spectral analysis

A. Theoretical development of cyclostationary analysis

A couple of definitions for a cyclostationary signal has been put forward [27]. Of relevance in this work is cyclostationarity of order 2, in which case then we are dealing with a quadratic transformation of the time signal. More specifically, a quadratic transformation of the type involving the product of a signal with a delayed version of itself, i.e. the autocorrelation function, will generate spectral lines. Thus, it means that a continuous signal $x(t)$ is cyclostationary of order two with fundamental cyclic frequency (or cycle frequency) α if and only if at least some of its delayed products namely $y(t) = x(t)x^*(t-\tau)$ for some delays τ exhibit a spectral line at this cyclic frequency α. The next important definition is the cyclic autocorrelation function (CAF) of a cyclostationary process which is defined as [27]:

$$r_{xx}^{\alpha_k}(t) = \frac{1}{T}\int_{-\frac{T}{2}}^{\frac{T}{2}} r_{xx}\left(t+\frac{t}{2}, t-\frac{t}{2}\right) \mathrm{e}^{-j2p\alpha_k t}\,\mathrm{d}t \qquad (1)$$

The spectral correlation density function (SCDF) or cyclic spectrum is the frequency domain representation of the CAF according to the Wiener-Khinchin relation and is given in continuous time as [27]:

$$S_{xx}^{\alpha_k}(f) = \int_{-\infty}^{\infty} r_{xx}^{\alpha_k}(t)\ \mathrm{e}^{-j2pft}\,\mathrm{d}f \qquad (2)$$

The Degree of Cyclostationarity (DCS) is basically a measure of the degree of non-stationarity for a wide-sense cyclostationary process and its value lies between zero and unity. It can be computed either from the CAF or from the SCDF, and using the latter is defined in continuous domain as [35]:

$$\mathrm{DCS}^{\alpha} = \frac{\int_{-\infty}^{\infty} |S_{xx}^{\alpha}(f)|^2\,\mathrm{d}f}{\int_{-\infty}^{\infty} |S_{xx}^{0}(f)|^2\,\mathrm{d}f} \qquad (3)$$

B. Procedures for analysis

Preliminary analysis using the cyclostationary analysis with the experimental setup in this paper has been done [36], [37]. Reference [37] looked into the statistical evidence of cyclostationary behaviour of the boring bar vibrations. The analysis however did not investigate the force modulation phenomenon that the boring bar experiences when in operation. The process of machining a workpiece on a lathe is usually time-varying; for example we have variation in cutting speed, feed rate, cutting depth, tool wear, etc. [38]. Thus, the cutting process in the lathe can normally be expected to exhibit a non-stationary character, i.e. a process with time-varying properties. However, assuming that throughout the cutting process the following conditions hold namely: no alteration of cutting data (i.e. cutting speed, feed rate and depth of cut), slow deterioration rate of the tool, and time-invariance of the basic structure of the work material, then the cutting forces can be hypothesised as short time stationary random processes. It is of importance to be able to identify these so-called stationary segments of the data because it enables the usage of the toolbox defined for stationary random processes to analyse the data. Two commonly available tests for stationarity that are used in this work are the reverse arrangement test and the run test [39].

A block size has to be calculated for the stationary tests. In Reference [3], a block size of 2400 samples to filter out the first eigenfrequency of the boring bar of about 600 Hz was identified. This can be explained as follows: With the knowledge of an approximate

value of 600 Hz for the first eigenfrequency (in either CSD or CDD) and a sampling frequency F_s of 48 kHz, it can be readily observed that, choosing a block size of 2400 samples, the number of periods of this 600-Hz-eigenfrequency is 30 (in this 2400 samples). This value of 30 averages was considered sufficient to average out the eigenfrequency effect and it is important to note that in order not to interfere with any other phenomenon (periodic or not) present in the data, it is essential not to use more averages than necessary. This block size of 2400 samples corresponds to an averaging time of 0.05 s. Amplitude-modulated vibration signals emanating from rotating machinery generally involve harmonics of the rotating component. It is obvious that if the spindle rotation frequency is filtered out by some averaging time, then so are its harmonics. A simple and most straightforward method to achieve this is to increase the block size (from the 2400 samples) until we cannot observe any fluctuating trend in the mean square values. The optimum block size, in this respect, to filter out the low spindle rotation frequency of around 6 Hz was found to be 96 000 samples, implying an averaging time of 2 s.

Cyclostationarity (in the wide sense) implies periodic variation in the second-order characteristics, hence in the mean square values also. Now from the previous paragraph, it is clear that using a block size of 96 000 samples filters or smoothes out any periodic fluctuations in the mean square values. Therefore, it is obvious that any stationary segments identified in the time data record will contain cyclostationary components as well. It is useful to note that since the two stationarity tests rest on the normal distribution assumption, the minimum number of observations has been set to a value of 10. Also here, it is useful to point out that the level of significance was set to 0.05 and this irrespective of the number of observations. A Matlab [40] script has been written, the purpose of which is to help identifying stationary segments in the time data records and identifying the longest possible stationary segment so that in the analysis, we are sure to obtain the most reliable spectral estimates, be it with the PSD or with the cyclic spectrum in the cyclostationary analysis.

1) Selection of vibration data for analysis

A suitable approach had to be found to identify data that will most probably be of interest in the cyclostationary analysis. The essential steps in this selection procedure for each of the boring bar vibration data were to:

1) Identify the longest stationary segment in the data using the reverse arrangement test and the run test.
2) Compute the PSD in a frequency region around the first eigenfrequency of the boring bar (which is around 600 Hz in either CDD or CSD) over this longest stationary segment.
3) In the event that the PSD from Step 2 displays sufficient amplitude-modulation phenomenon (in the form of sidebands in the frequency region around the eigenfrequency), then the boring bar vibration data is considered as a potential candidate for cyclostationary analysis.

Having identified potential candidates for analysis, the next step was to compute the DCS function. The DCS function is expected to exhibit sufficient energy at α other than zero at twice the low spindle rotation frequency and also at high frequencies around twice the first eigenfrequency (assuming that these two frequency components are mainly responsible for the vibration of the boring bar). If the DCS does not show these features, the vibration data is discarded. It was not timely possible to investigate each of the boring bar vibration data, but it has been found in general that data with the highest primary feed rate of $s = 0.3$ mm/rev had the desired features. In this respect, data pertaining to this high feed-rate was investigated for various cutting speeds and for the three different workpiece materials mentioned in Table II, and the normalised random error was computed according to Reference [27].

2) Estimation of PSD

The Welch method [41] has been used for the computation of the PSD. The p^{th} periodogram of length N_1 with the use of windows is given by

$$\hat{I}_{xx}^{p}\left(f_k\right) = \frac{T_s}{N_1\, U}\left|\sum_{i=0}^{N_1-1} x_p(i)\, w(i) e^{-j\frac{2\,p\,k\,n}{N_1}}\right|^2, \quad 0 \le p \le N_2 - 1 \tag{4}$$

where f_k is given by $f_k = \frac{k}{N_1\, T_s}$ and

$$U = \frac{1}{N_1}\sum_{n=0}^{N_1-1}\left(w(n)\right)^2 \tag{5}$$

is the window-dependent resolution bandwidth normalisation factor [42] for PSD estimation. Finally, the Welch estimate, $\hat{I}_{xx}$, is the average of all the periodograms over all segments N_2 as follows:

$$\hat{I}_{xx}\left(f_k\right) = \frac{1}{N_2}\sum_{p=0}^{N_2-1} I_{xx}^{(p)}\left(f_k\right) \tag{6}$$

3) Estimation of SCDF in discrete time

The estimation method that has been adopted is the cyclic correlogram method [43]. Its formulation involves estimation of the CAF, $\hat{r}_{xx}(\alpha,\, m)$, and then of the SCDF, $\hat{S}_{xx}(\alpha,\, f)$, as shown in Fig. 3 and the estimators are provided in Equation (7).

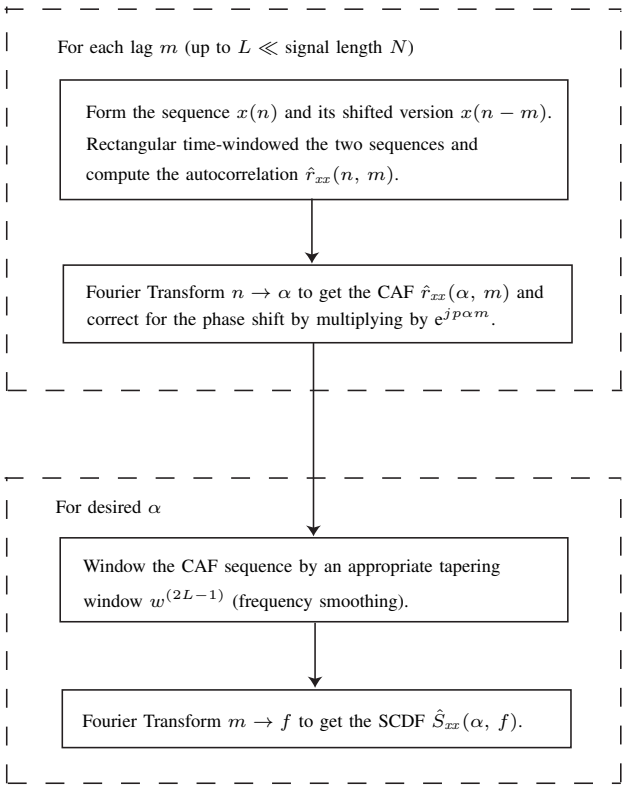

Fig. 3. Schematic representation of the estimation of the SCDF via the cyclic correlogram method. See also Equation (7)

The discrete time estimators for the CAF, $\hat{r}_{xx}(\alpha,\, m)$, and for the SCDF, $\hat{S}_{xx}(\alpha,\, f)$, [43] are given next in Equation (7):

$$\hat{r}_{xx}(\alpha_k,\, m) \;=\; \frac{1}{N}\sum_{n=0}^{N-1} x(n)\, x^*(n-m)\, \mathrm{e}^{-j2p\alpha_k n}\, \mathrm{e}^{jp a_k m} \tag{7a}$$

$$\hat{S}_{xx}(\alpha_k,\, f_k) = \frac{1}{N}\sum_{m=-L}^{L} w^{(2L-1)}(m)$$

$$\left[x(n)x^*(n-m)\,\mathrm{e}^{-j2p\alpha_k n}\,\mathrm{e}^{jp\alpha_k m}\right]\mathrm{e}^{\frac{-j2pkm}{2L+1}} \quad (7b)$$

with the cyclic frequency $\alpha_k = k\,\frac{1}{T_s}$, $k = 0, \pm1, \pm2, \ldots$ and $\frac{1}{T_s}$ is the fundamental frequency. It is readily apparent that when $\alpha_k = 0$, Equation (7a) reduces to the conventional autocorrelation function. Also, then a generally non-stationary process is said to exhibit cyclostationarity in the wide sense only if there exists correlation between some frequency-shifted versions of the process as opposed to a stationary process which exhibits no correlation between any frequency-shifted versions of the process.

In the computation of the CAF, a rectangular window was applied to the time shifted sequences. Similarly, in the computation of the SCDF (see Equation (7b)), a suitable window needs to be applied prior taking the Fourier Transform with respect to m. A symmetric window with tapering ends and having unity magnitude at $m = 0$ has the advantage of de-emphasising the unreliable parts of the CAF, thus reducing the variance in the computation of the SCDF. Thus in Equation (7b), the window w, with support $[-L,\, L]$ and of length $2L - 1$, is applied to the CAF sequence which has been calculated using Equation (7a) for both positive and negative lags k. The negative CAF values are obtained from the positive counterparts by exploiting the symmetry property of the CAF.

The PSD and SCDF estimation parameters are presented in Tables III and IV respectively. Of importance is to note that one optimisation made on the SCDF estimation code was to downsample the data and hence the sampling frequency F_s (from 48 kHz to 3 kHz). The resulting theoretical useful frequency range up to 1.5 kHz still encompasses the frequency region of interest in both axes of the SCDF bi-frequency plane. Statistical measures of the PSD and the SCDF are given in Tables III and V respectively. The normalised random error ε_r is also known as the coefficient of variation and is commonly used in spectral analysis [44]. Window characteristics are assessed using two important criteria, namely the equivalent noise bandwidth, B_e which provides a measure of the bandwidth of the window in the frequency domain [45] and the statistical bandwidth, B_s, which is also a measure of window bandwidth [44]. In Table V, the following relationship holds [27]:

$$\varepsilon_r \simeq \sqrt{\frac{B_e}{B_s}} \quad (8)$$

TABLE III
Parameters for PSD estimation

Parameter	Value
Data length (samples)	Longest stationary segment
Sampling frequency F_s [kHz]	48
Periodogram's length (samples)	65 536
Time window	Hanning
Overlapping [%]	50
Normalised random error, ε_r	0.1072–0.1387

TABLE IV
Parameters for SCDF estimation

Parameter	a-direction	f-direction
Original data length (samples)	819 200	32 768
Downsampled data length (samples)	51 200	2048
Window	Rectangular	Bartlett

TABLE V
Statistical measures of the SCDF

Parameter	Value
Equivalent noise bandwidth, B_e	0.0781
Statistical bandwidth, B_s	2.1973
Normalised random error, ε_r	0.1886

IV. Results

Many of the data analysed had common features and the objective here is to give representative results either in CDD or in CSD. The parameters for the spectral analyses are based on Tables III to V in Section III-B3. The analysis results are presented in the following order: PSD estimates in the high frequency region (around the first eigenfrequency of the boring bar) and in the low frequency region (encompassing the spindle rotation frequency), and the SCDF contour plots at low cyclic frequencies but at high (spectral) frequencies and at high cyclic frequencies but at low (spectral) frequencies. Accompanying these SCDF contour plots are the DCS functions which facilitate the observation of the spectral correlation features. The results that follow next are for the three materials listed in Table II. Of importance is to note that the SCDF estimates were scaled for the random component and the corresponding SCDF contour plots in Matlab [40] had a level of detail set at 150. Also there were no significant differences between results in the cutting depth direction and in the cutting speed direction.

A. Workpiece material SS 0727-02

This section presents the results for material SS 0727-02. For the vibration data in CDD with $v = 175$ m/min and $s = 0.3$ mm/rev, Fig. 4 shows respectively the PSD estimate of the data in the high frequency and in the low frequency regions, and the SCDF contour plots are given in Fig. 5 for the low cyclic frequency region around twice the spindle rotation frequency and for the high cyclic frequency region at around twice the first eigenfrequency respectively. Figures 6 and 7 show the corresponding results for the vibration data in CDD with $v = 225$ m/min and $s = 0.3$ mm/rev.

B. Workpiece material SS 2343-02

This section presents the results for material SS 2343-02 for vibration data in CSD with $v = 150$ m/min and $s = 0.3$ mm/rev. Figure 8 shows respectively the PSD estimate of the data in the high frequency and in the low frequency regions. The SCDF contour plots are given in Fig. 9 for the low cyclic frequency region around twice the spindle rotation frequency and for the high cyclic frequency region at around twice the first eigenfrequency respectively.

C. Workpiece material SS 2541-03

This section presents the results for material SS 2541-03 for vibration data in CDD with $v = 225$ m/min and $s = 0.3$ mm/rev. Figure 10 shows respectively the PSD estimate of the data in the high frequency and in the low frequency regions. The SCDF contour plots are given in Fig. 11 for the low cyclic frequency region around twice the spindle rotation frequency and for the high cyclic frequency region at around twice the first eigenfrequency respectively.

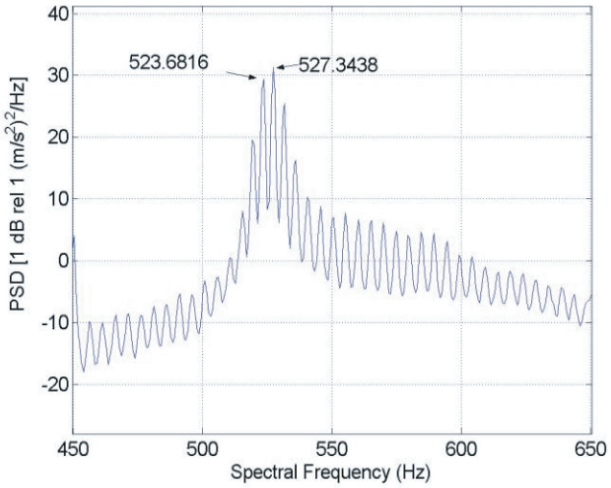

(a) PSD estimate in high frequency region

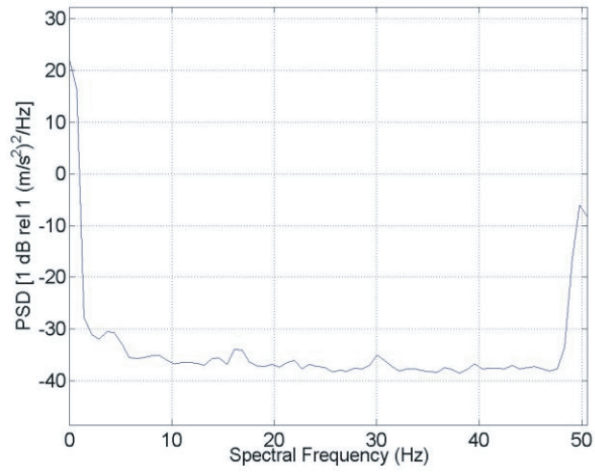

(b) PSD estimate in low frequency region

Fig. 4. PSD estimates in the high frequency region (top figure) and low frequency region (bottom figure) of the dynamic response of the boring bar in the cutting depth direction during a continuous cutting operation in material SS 0727-02, feed rate $s = 0.3$ mm/rev, cutting depth $a = 2$ mm, cutting speed $v = 175$ m/min, tool DNMG 150608-SL and grade TN7015. The number of periodogram averages was 87. The separation of the peaks is approximately 3.66 Hz in the top figure

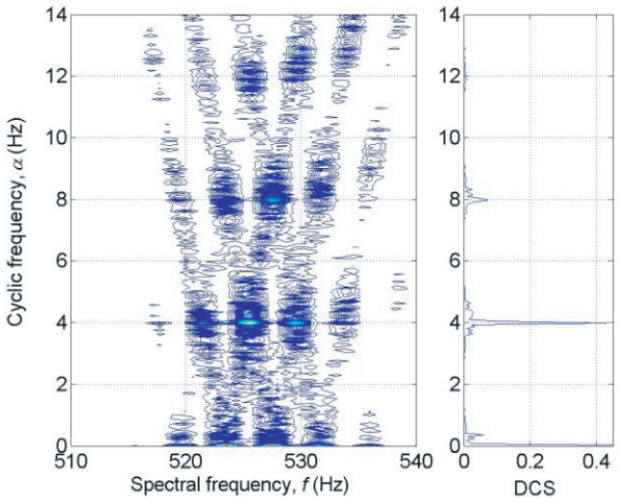

(a) PSD estimate in high frequency region

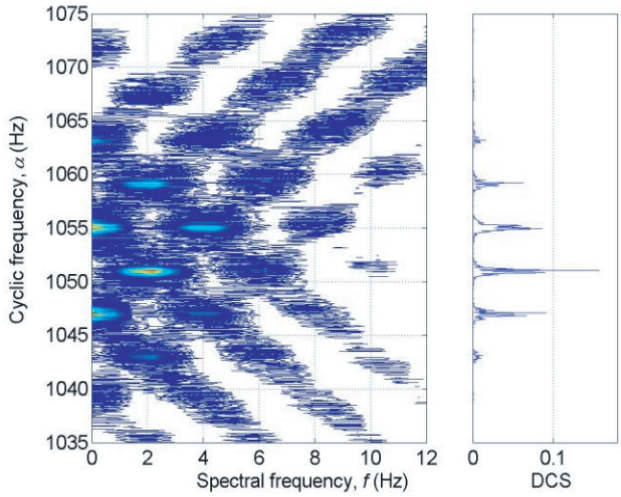

(b) PSD estimate in low frequency region

Fig. 5. The SCDF contour plots alongside with DCS functions of the dynamic response of the boring bar in the cutting depth direction during a continuous cutting operation in SS 0727-02, feed rate $s = 0.3$ mm/rev, cutting depth $a = 2$ mm, cutting speed $v = 175$ m/min, tool DNMG 150608-SL and grade TN7015. Top figure: low cyclic frequencies and high spectral frequencies; observe the two peaks in the DCS function at $\alpha = 3.9844$ Hz and 7.9688 Hz. Bottom figure: high cyclic frequencies and low spectral frequencies; observe the main peak in the DCS function at $\alpha = 1051.05$ Hz (around twice the 600 Hz eigenfrequency value)

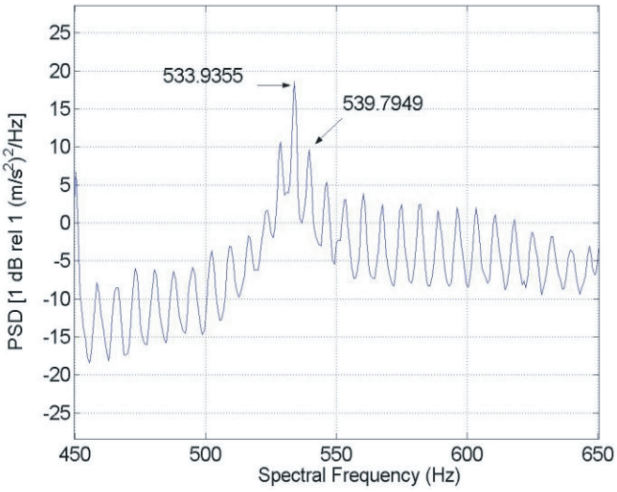

(a) PSD estimate in high frequency region

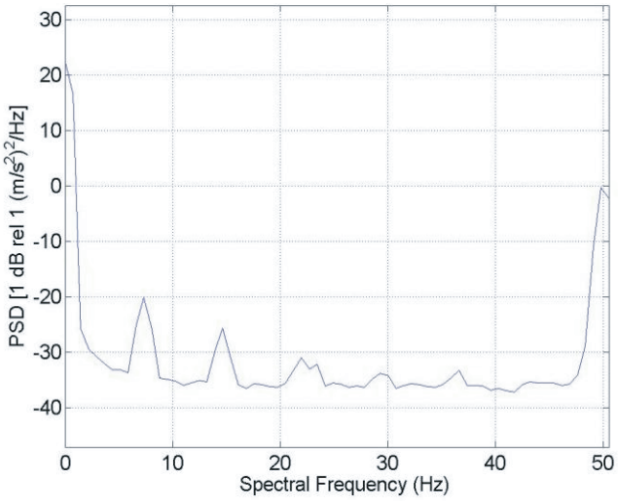

(b) PSD estimate in low frequency region

Fig. 6. PSD estimates in the high frequency region (top figure) and low frequency region (bottom figure) of the dynamic response of the boring bar in the cutting depth direction during a continuous cutting operation in material SS 0727-02, feed rate $s = 0.3$ mm/rev, cutting depth $a = 2$ mm, cutting speed $v = 225$ m/min, tool DNMG 150608-SL and grade TN7015. The number of periodogram averages was 75. The separation of the peaks is approximately 5.86 Hz in the top figure

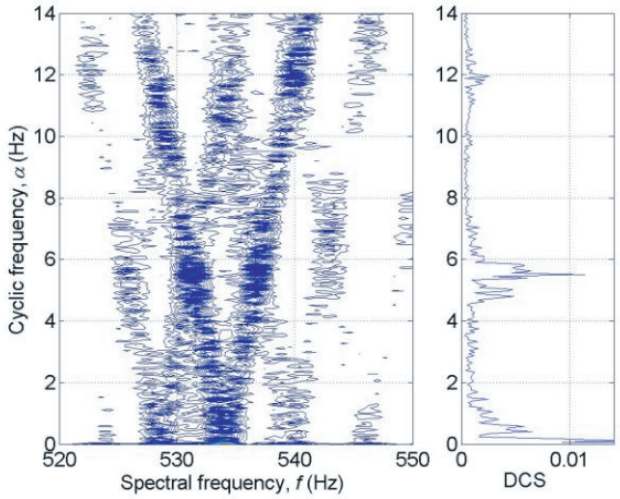

(a) PSD estimate in high frequency region

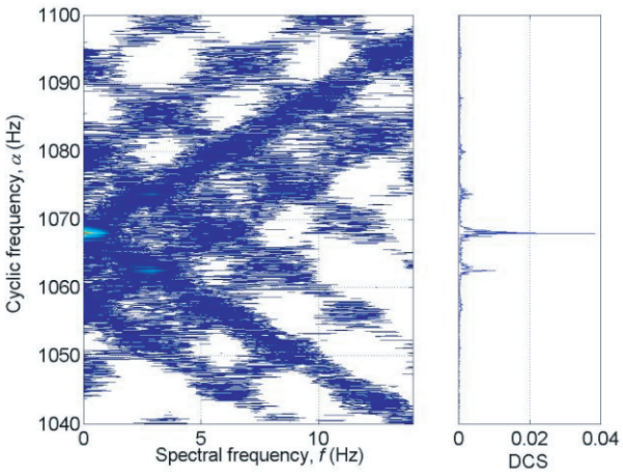

(b) PSD estimate in low frequency region

Fig. 7. The SCDF contour plots alongside with DCS functions of the dynamic response of the boring bar in the cutting depth direction during a continuous cutting operation in SS 0727-02, feed rate $s = 0.3$ mm/rev, cutting depth $a = 2$ mm, cutting speed $v = 225$ m/min, tool DNMG 150608-SL and grade TN7015. Top figure: low cyclic frequencies and high spectral frequencies; observe the main peak in the DCS function at $\alpha = 5.5078$ Hz. Bottom figure: high cyclic frequencies and low spectral frequencies; observe the main peak in the DCS function at $\alpha = 1067.99$ Hz (around twice the 600 Hz eigenfrequency value)

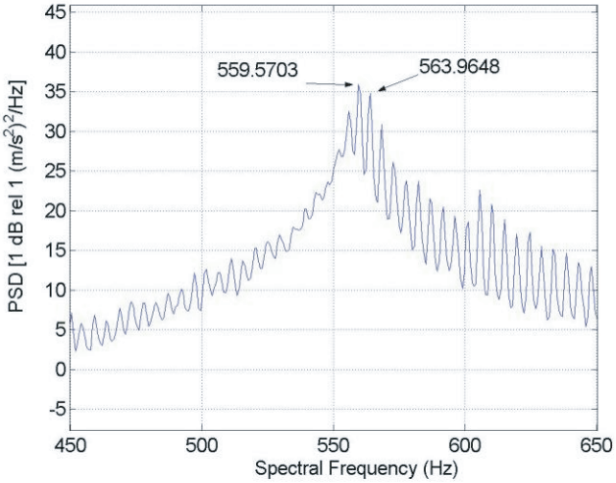

(a) PSD estimate in high frequency region

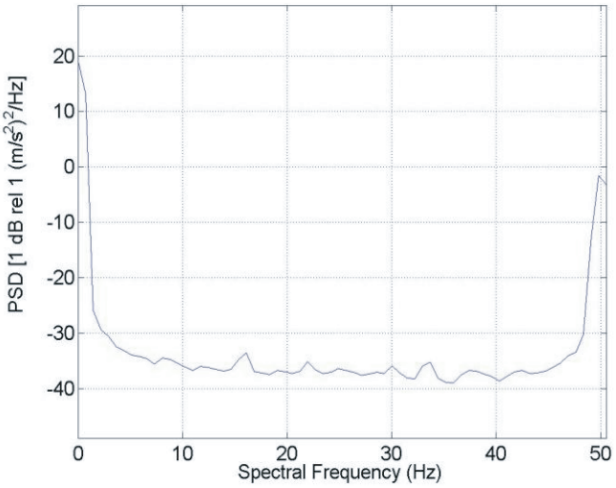

(b) PSD estimate in low frequency region

Fig. 8. PSD estimates in the high frequency region (top figure) and low frequency region (bottom figure) of the dynamic response of the boring bar in the cutting speed direction during a continuous cutting operation in material SS 2343-02, feed rate $s = 0.3$ mm/rev, cutting depth $a = 2$ mm, cutting speed $v = 150$ m/min, tool DNMG 150608-SL and grade TN8025. The number of periodogram averages was 87. The separation of the peaks is approximately 4.4 Hz in the top figure

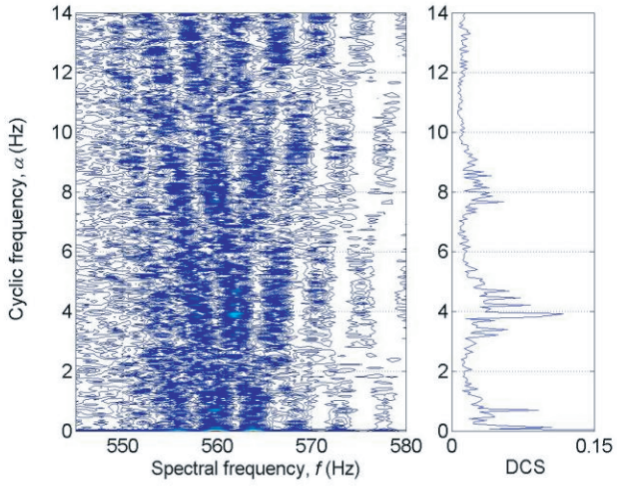

(a) PSD estimate in high frequency region

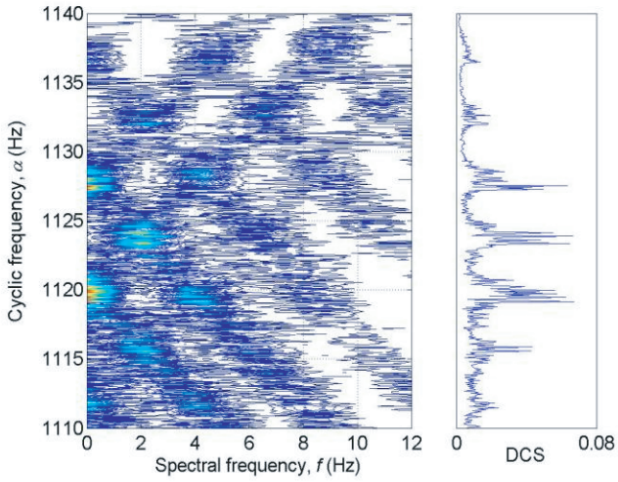

(b) PSD estimate in low frequency region

Fig. 9. The SCDF contour plots alongside with DCS functions of the dynamic response of the boring bar in the cutting speed direction during a continuous cutting operation in SS 2343-02, feed rate $s = 0.3$ mm/rev, cutting depth $a = 2$ mm, cutting speed $v = 150$ m/min, tool DNMG 150608-SL and grade TN8025. Top figure: low cyclic frequencies and high spectral frequencies; observe the main peak in the DCS function at $\alpha = 3.9258$ Hz. Bottom figure: high cyclic frequencies and low spectral frequencies; observe the three main peaks in the DCS function at $\alpha = 1119.14$ Hz, 1123.89 Hz and 1127.52 Hz (around twice the 600 Hz eigenfrequency value)

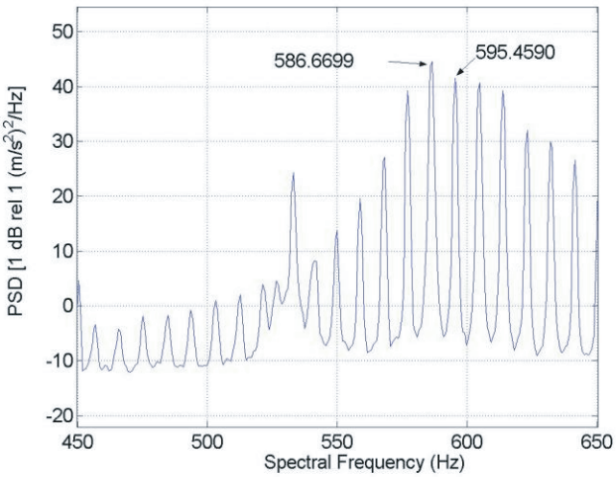

(a) PSD estimate in high frequency region

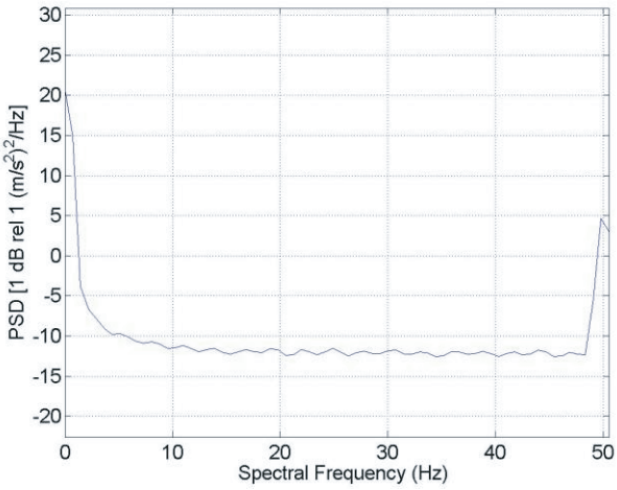

(b) PSD estimate in low frequency region

Fig. 10. PSD estimates in the high frequency region (top figure) and low frequency region (bottom figure) of the dynamic response of the boring bar in the cutting depth direction during a continuous cutting operation in material SS 2541-03, feed rate $s = 0.3$ mm/rev, cutting depth $a = 2$ mm, cutting speed $v = 225$ m/min, tool DNMG 150608-SL and grade TN7015. The number of periodogram averages was 87. The separation of the peaks is approximately 8.79 Hz in the top figure

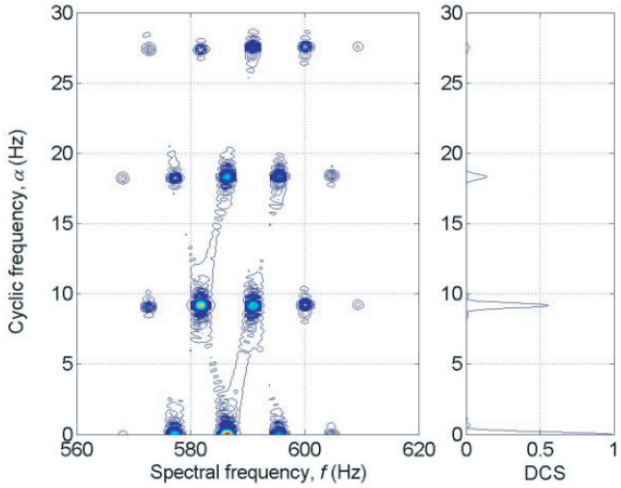

(a) PSD estimate in high frequency region

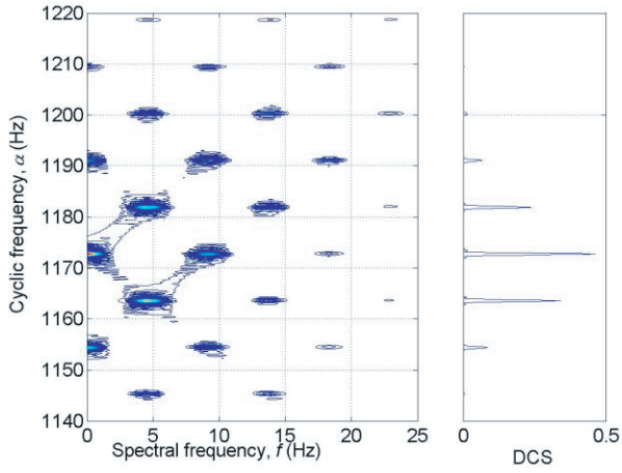

(b) PSD estimate in low frequency region

Fig. 11. The SCDF contour plots alongside with DCS functions of the dynamic response of the boring bar in the cutting depth direction during a continuous cutting operation in SS 2541-03, feed rate $s = 0.3$ mm/rev, cutting depth $a = 2$ mm, cutting speed $v = 225$ m/min, tool DNMG 150608-SL and grade TN7015. Top figure: low cyclic frequencies and high spectral frequencies; observe the main peak in the DCS function at $\alpha = 9.1992$ Hz. Bottom figure: high cyclic frequencies and low spectral frequencies; observe the three main peaks in the DCS function at $\alpha = 1163.61$ Hz, $\alpha = 1172.70$ Hz and 1181.89 Hz respectively (around twice the 600 Hz eigenfrequency value)

V. Discussions and Analyses

In the PSD estimates of the boring bar vibration data, there seems to be a correlation between the adjacent sideband distance and the workpiece rotation frequency. This might suggest that workpiece motion at the rotation frequency amplitude modulates the response of the boring bar at its first eigenfrequency.

Two types of amplitude modulation phenomena are principally observed in the data for the three materials considered in the analysis. One type is observed for the material SS 0727-02 in Figs 4 and 5, and for the material SS 2343-02 in Figs 8 and 9. If amplitude modulation is assumed, this modulation might for instance explain the cyclic spectrum in Fig. 5 at the cyclic frequency of $\alpha = 3.9844$ Hz. If it is assumed that we have the eigenfrequency in the cutting depth direction at $\frac{1051.05}{2} \simeq 525.525$ Hz, then this may be described by the following amplitude modulation model:

$$x(n) = \left[1 + \sin\left(2\,\pi\,\frac{1051.05}{2}\;n\right)\right] \times \left[\sin\left(2\,\pi\,\frac{3.9844}{2}\;n\right) + \sin\left(2\,\pi\;\times\;3\;\times\;\frac{3.9844}{2}\;n\right) + \ldots\right] \tag{9}$$

where $x(n)$ is the vibration signal. This model suggests an amplitude modulation of half the spindle rotation frequency.

The second type of amplitude modulation is observed for the material SS 0727-02 in Figs 6 and 7, and for material SS 2541-03 in Figs 10 and 11. Considering for instance Fig. 7 where the eigenfrequency in the cutting depth direction is $1067.99/2$ Hz and the fundamental cyclic frequency is 5.5078 Hz, the modulation pattern can be assumed to be of the form

$$x(n) = \left[1+\sin\left(2\,\pi\,5.5078\,n\right)+\sin\left(2\,\pi\;\times\;2\;\times\;5.5078\,n\right)+\ldots\right] \times \left[\sin\left(2\,\pi\,\frac{1067.99}{2}\;n\right)\right] \tag{10}$$

where $x(n)$ is the vibration signal. Here on the other hand, an amplitude modulation with the actual spindle rotation frequency is indicated. It is to be noted that in both Equations 9 and 10 element-wise multiplication is implied at the discrete time index n.

Next, variations in the peaks at the fundamental cyclic frequency are observed in the DCS functions accompanying the SCDF contour plots for the materials SS-0727-02 and SS 2343-02 (both with $s = 0.3$ mm/rev). This can be observed e.g. in Fig. 9. This variation implies a change in the cutting speed v occurring in the metal cutting process. This variation in frequency is known as frequency modulation. Furthermore, this results in spreading of energy to the surrounding peaks in the DCS function. On the other hand, this frequency modulation effect was observed to be much less severe for the material SS 2541-03. Besides it was found for this material that these frequency variations tend to disappear with higher cutting speeds. This is seen in Fig. 11 where one can observe that the peaks in the DCS function are well-defined. This cannot be explained by the resistance of the workpiece materials during the cutting process since material SS 0727-02 is cast iron whereas materials SS 2343-02 and SS 2541-03 are steel-based. Examining the contour SCDF plots alongside with the DCS functions allows one to resolve the type of amplitude modulation pattern present and this information is not readily available from a PSD estimate.

Furthermore, for a given amplitude modulation type, the size of the rhombic spectral correlation patterns of the SCDF plots in the bi-frequency SCDF plane is dictated by their cyclic frequencies, the first eigenfrequency in CSD or CDD and possibly the cutting speed v. The low frequency modulating component appears to be the spindle rotation frequency. It is to be expected that the cyclic frequency is twice the spindle rotation frequency (considering the relationship of the cyclic frequency α to the spectral frequency f). Indeed, Reference [46] in the application of cyclostationary analysis to study bearings showed that this low modulating cyclic frequency can be in fact related to the rotation frequency of the bearing or to some bearing's fault such as an inner race fault, or to both of them. In this work, it is thus expected that the low cyclic frequency components observed in all of the vibration data has some direct relationship to the spindle rotation frequency.

Hence, after having found that second-order cyclostationary analysis can identify the modulation phenomenon present in the vibration data, a next crucial step is to identify the nature of the cyclic frequency components. To that end, the rotation speed was calculated (based on the workpiece diameter and the cutting speed) and compared to the cyclic frequency for each data. The workpiece diameter considered here is the diameter at the start of the cutting process. Table VI shows this comparison.

TABLE VI. Comparison of spindle rotation frequency with cyclic frequency

Vibration data[1]	Starting workpiece diameter [m]	Rotation frequency based on Column 2 [Hz]	Observed α in Section IV [Hz]	% magnitude difference between Columns 3 and 4 based on Column 4
Workpiece material SS 0727-02 (with $s = 0.3$ mm/rev)				
CDD—175	0.2000	4.6420	3.9844	16.50
CDD—225	0.1750	6.8209	5.5078	23.84
CSD—275	0.1900	7.6785	6.2695	22.47
Workpiece material SS 2343-02 (with $s = 0.3$ mm/rev)				
CDD—75	0.1662	2.3940	3.0469	21.43
CSD—150	0.1793	4.4382	3.9258	13.08
Workpiece material SS 2541-03 (with $s = 0.3$ mm/rev)				
CDD—225	0.1380	8.6497	9.1992	5.97

[1] *The numerical value after CDD or CSD refers to the cutting speed v m/min*

It can be seen from Table VI that there is a relatively small difference for the material SS 2541-03 (with $s = 0.3$ mm/rev). Although not shown here, the author has been able to find that this difference was in fact lower than 15 % for the other seven cutting data (three in the CDD and four in the CSD) for this material. The discrepancies are more severe for the materials SS 2343-02 and SS 0727-02. The diameters of the workpiece materials were measured by the CNC coordinate system in the lathe. Now, for each new insert the position of the tool tip is not calibrated so that in effect, it can be said that the coordinate system only provides us with an approximate value of the diameter of the workpiece. This leads to the conclusion that the spindle rotation frequencies calculated in Column 3 of Table VI represent in fact approximations to the true spindle rotation frequencies. It is also important here to take into account the frequency modulation effect observed in the data for the steel-based material SS 2343-02 and cast iron material SS 0727-02.

The true spindle rotation frequencies are in most cases observable from the PSD estimates at the lower frequencies. Based on the preceding discussions, it can be put forward that the spindle rotation frequency is in fact the cyclic frequency as observed in the SCDF plots. This leads us to think of some other phenomenon affecting the cutting process. In fact, in rotating machinery, it is not

uncommon to observe that looseness in some fixtures manifests itself by a sideband at half the rotation frequency of the main rotating component [47]. The fact that the cutting speed varies during cutting and that the SCDF plots suggest either an amplitude modulation of the eigenfrequency with half the workpiece rotation frequency or with the actual workpiece rotation frequency leads to the conclusion that the structure of the boring bar vibration is more complex than the hypothesised simple amplitude modulation structure.

VI. Conclusions

The objective of this work is to investigate the force modulation phenomenon associated with the dynamic motion of the boring bar in the metal cutting process on a lathe. In Reference [3] it has been shown that the effect of the material deformation process is to induce vibration in the boring bar at the first eigenfrequency in either CDD or CSD. Unbalance in the workpiece rotation was also known to affect the vibrations of the boring bar. The stochastic nature of the cutting process is exposed by the PSD analysis, but the latter is limited in analysis by its time-invariance property.

As seen in Sections IV and V, the PSD analysis has proved to be not quite effective in revealing whether there is modulation phenomenon occurring in the vibration data nor the exact form in case of occurrence of amplitude modulation. In the second-order cyclostationary analysis, the DCS function serves as preliminary tool to unveil the presence of modulation in the vibration data. Also, in-depth analysis with the SCDF bi-frequency contour plots could, in every case considered, provide concise and unambiguous information regarding the amplitude modulation phenomenon occurring. The DCS function could be computed separately before computing the SCDF which is more computationally expensive.

The results obtained in Section IV indicate that the cyclic spectrum (or SCDF plot) is likely to provide information concerning the frequency of the actual boring bar eigenfrequency from the force-modulated boring bar vibration data. Moreover, the cyclostationary analysis unwrapped new information from the cutting process. Firstly, the cycle frequencies obtained from the analysis may indicate the presence of looseness in the fixture of the boring bar. Secondly, frequency variations in the peaks of the DCS functions were observed for the materials SS 2343-02 (steel-based) and SS 0727-02 (cast iron). This variation in the DCS peaks leads to the phenomenon of frequency modulation, which has not been investigated further in this work. It is known that the cutting speed varies during cutting and this coupled to the fact that the cyclostationary analysis suggests either an amplitude modulation of the eigenfrequency with half the workpiece rotation frequency or with the actual workpiece rotation frequency, shows that the amplitude modulation models put forward in Section V may not be complete.

The manufacturing industry is always putting much effort to reduce the vibration emanating from the metal cutting process on a lathe. Thus, understanding the causes and sources of the vibration causing effect is fundamental. In this work, second-order cyclostationary analysis has revealed some looseness in the boring bar fixture; such information is vital to the vibration control engineers. In essence, cyclostationary analysis at the second order has demonstrated its ability to handle the non-stationary stochastic nature of the metal cutting process on a lathe.

Acknowledgments

The author wishes to express his sincere thanks to Prof. Lars Håkansson of the Department of Applied Signal Processing, Blekinge Tekniska Högskola (Blekinge Institute of Technology), Sweden, for his assistance.

References

[1] Y. Altintas. *Manufacturing Automation, Metal Cuting Mechanics, Machine Tool Vibrations, and CNC design*. Cambridge University Press, 2000.

[2] L. Håkansson. *Adaptive Active Control of Machine-Tool Vibration in a Lathe—Analysis and Experiments*. PhD thesis, Department of Production and Materials Engineering, Lund University, Sweden, 1999.

[3] L. Pettersson. *Vibrations in metal cutting: measurement, analysis and reduction.* Licentiate thesis, Department of Telecmmunications and Signal Processing, Blekinge Institute of Technology, Sweden, 2002.

[4] J. Tlusty. Analysis of the state of research in cutting dynamics. In *Annals of the CIRP*, volume 27/2, pages 583–589. CIRP, 1978.

[5] D.W. Wu and C.R. Liu. An analytical model of cutting dynamics—Part 1: Model building. *Journal of Engineering for Industry, Transactions of the ASME*, 107(2):107–111, May 1985.

[6] D.W. Wu and C.R. Liu. An analytical model of cutting dynamics—Part 2: Verification. *Journal of Engineering for Industry, Transactions of the ASME*, 107(2):112–118, May 1985.

[7] I.E. Minis, E.B. Magrab, and I.O. Pandelidis. Improved methods for the prediction of chatter in turning—Part 1: Determination of structural response parameters. *Journal of Engineering for Industry, Transactions of the ASME*, 112:12–20, February 1990.

[8] I.E. Minis, E.B. Magrab, and I.O. Pandelidis. Improved methods for the prediction of chatter in turning—Part 2: Determination of cutting process parameters. *Journal of Engineering for Industry, Transactions of the ASME*, 112:21–27, February 1990.

[9] I.E. Minis, E.B. Magrab, and I.O. Pandelidis. Improved methods for the prediction of chatter in turning—Part 3: A generalized linear theory. *Journal of Engineering for Industry, Transactions of the ASME*, 112:28–35, February 1990.

[10] S.M. Pandit, T.L. Subramanian, and S.M. Wu. Modeling machine tool chatter by time series. *Journal of Engineering for Industry, Transactions of the ASME*, 97:211–215, February 1975.

[11] S.M. Pandit, T.L. Subramanian, and S.M. Wu. Stability of random vibrations with special reference to machine tool chatter. *Journal of Engineering for Industry, Transactions of the ASME*, 97:216–219, February 1975.

[12] T. Kalmár-Nagy, G. Stépán, and F.C. Moon. Subcritical Hopf bifurcation in the delay equation model for machine tool vibrations. *Journal of Nonlinear Dynamics*, 26:121–142, 2001.

[13] J. Gradišek, E. Govekar, and I. Grabec. Chatter onset in non-regenerative cutting: A numerical study. *Journal of Sound and Vibration*, 242(5):829–838, 2001.

[14] E.W. Parker. Dynamic stability of a cantilever boring bar with machined flats under regenerative cutting conditions. *Journal of Mechanical Engineering Sience*, 12(2):104–115, February 1970.

[15] G.M. Zhang and S.G. Kapoor. Dynamic modeling and analysis of the boring machining system. *Journal of Engineering for Industry, Transactions of the ASME*, 109(3):219–226, August 1987.

[16] P.N. Rao, U.R.K. Rao, and J.S. Rao. Towards improwed design of boring bars—Part 1: Dynamic cutting force model with continuous system analysis for the boring bar. *International Journal of Machine Tools and Manufacture*, 28(1):33–44, 1988.

[17] F. Kuster and P.E. Gygax. Cutting dynamics and stability of boring bars. *CIRP Annals—Manufacturing Technology*, 39(1):361–366, 1990.

[18] S. Jayaram and M. Iyer. An analytical model for prediction of chatter stability in boring. *SME technical paper, (MR00-202), Society of Manufacturing Engineers*, 28:203–208, 2000.

[19] I. Lazoglu, F. Atabey, and Y. Altintas. Dynamics of boring processes—Part III: Time domain modeling. *International Journal of Machine Tools & Manufacture*, 42:1567–1576, 2002.

[20] M.K. Khraisheh, C. Pezeshki, and A.E. Bayoumi. Time series based analysis for primary chatter in metal cutting. *Journal of Sound and Vibration*, 180(1):67–87, 1995.

[21] P-O. H. Sturesson, L. Håkansson, and I. Claesson. Identification of the statistical properties of the cutting tool vibration in a continuous turning operation—Correlation to structural properties. *Mechanical Systems and Signal Processing*, 11(3):459–489, 1997.

[22] J. Gradišek, I. Grabec, S. Siegert, and R. Friedrich. Stochastic dynamics of metal cutting: Bifurcation phenomena in turning. *Mechanical Systems and Signal Processing*, 16(5):831–840, 2002.

[23] E. Marui, S. Ema, and S. Kato. Chatter vibration of lathe tools—Part 1: General characteristics of chatter vibration. *Journal of Engineering for Industry, Transactions of the ASME*, 105(2):100–106, May 1983.

[24] L. Andrén, L. Håkansson, A. Brandt, and I. Claesson. Identification of dynamic properties of boring bar vibrations in a continuous boring operation. *Mechanical Systems & Signal Processing*, 18(4):869–901, 2004.

[25] L. Andrén, L. Håkansson, A. Brandt, and I. Claesson. Identification of motion of cutting tool vibration in a continuous boring operation—Correlation to structural properties. *Mechanical Systems & Signal Processing*, 18(4):903–927, 2004.
[26] A. McCormick and A.K. Nandi. Cyclostationarity in rotating machine vibrations. *Mechanical Systems and Signal Processing*, 12(2):225–242, 1998.
[27] W.A. Gardner. *Statistical Spectral Analysis: A Non-Probabilistic Theory*. Prentice Hall, Englewood Cliffs, New York, 1987.
[28] C. Capdessus, Sidahmed. M., and J.L. Lacoume. Cyclostationary processes: Application in gear faults early diagnosis. *Mechanical Systems and Signal Processing*, 14(3):371–385, 2000.
[29] L. Bouillaut and M. Sidahmed. Cyclostationary approach and bilinear approach: comparison, applications to early diagnosis for helicopter gearbox and classification method based on HOCS. *Mechanical Systems and Signal Processing*, 15(5):923–943, 2001.
[30] R.B. Randall, J. Antoni, and S. Chobsaard. The relationship between spectral correlation and envelope analysis for cyclostationary machine signals, application to ball bearing diagnostics. *Mechanical Systems and System Processing*, 15(5):945–962, 2001.
[31] J. Antoni, J. Danière, and F. Guillet. Effective vibration analysis of IC engines using cyclostationarity—Part I: A methodology for condition monitoring. *Journal of Sound and Vibration*, 257(5):815–837, 2002.
[32] M. knaak and D. Filbert. Acoustical semi-blind source separation for machine monitoring. In *Proc. conference Indep. Compon. Anal. Signal*, pages 361–366, 2001.
[33] J. Goerlich, D. Bruckner, A. Richter, O. Strama, R.S. Thomä, and U. Trautwein. Signal analysis using spectral correlation measurement. In *IEEE Instrumentation and Measurement Technology Conference, St. Paul, U.S.A*, volume 2, pages 1313–1318, May 18–21 1998.
[34] Sandvik. General turning. Sandvik AB Coromant, [Online]. http://www2.coromant.sandvik.com/coromant/pdf/Metalworking_Products_061/tech_a_8.pdf.
[35] W.A. Gardner and G.D. Zivanovic. Degrees of cyclostationarity and their application to signal detection and estimation. *Signal Processing*, 22(3):287–297, 1991.
[36] Y. Calleecharan. Cyclostationary analysis of boring bar vibration. Master's thesis, Blekinge Institute of Technology, Sweden, ISRN: BTH-IMA-EX–2003/D-01–SE, January 2003.
[37] A.H. Brandt, L. Håkansson, and I. Claesson. Cyclostationary analysis of boring bar vibrations. In *IMAC-XXII: Conference & Exposition on Structural Dynamics*. Society of Experimental Mechanics, 2004.
[38] Sandvik. *Modern Metal Cuting: A Practical Handbook*. AB Sandvik Coromant, 1994.
[39] J.S. Bendat and A.G. Piersol. *Random data: Analysis and Measurement Procedures*. John Wiley & Sons, second edition, 1986.
[40] Matlab computing software, The MathWorks 2002. Version 6.5 (R13).
[41] P.D. Welch. The use of Fast Fourier Transform for the estimation of power spectra: A method based on time averaging over short, modified periodograms. *IEEE Transactions on Audio and Electroacoustics*, Au-15(2):70–73, June 1967.
[42] F. Harris. On the use of windows for harmonic analysis with the discrete Fourier Transform. In *Proc. of the IEEE*, volume 66, pages 51–83, 1978.
[43] W.A. Gardner. *Cyclostationarity in Communications and Signal Processing*. IEEE Press, New Jersey, 1994.
[44] J.S. Bendat and A.G. Piersol. *Random Data: Analysis and Measurement Procedures*. John Wiley & Sons, third edition, 2000.
[45] H. Jokinen, J. Ollila, and O. Aumala. On windowing effects in estimating averaged periodograms of noisy signals. *Measurement*, 28:197–207, 2000.
[46] I. Antoniadis and G. Glossiotis. Cyclostationary analysis of rolling-element bearing vibration signals. *Journal of Sound and Vibration*, 190(3):419–447, 1996.
[47] V. Wowk. *Machinery Vibration: Measurement and Analysis*. McGraw-Hill, 1991.

BIOGRAPHY

Yogeshwarsing Calleecharan received the B.Eng. (Hons) degree in Mechanical Engineering from the University of Mauritius, Mauritius, in 2000, the M.Sc. degree in Mechanical Engineering from Blekinge Tekniska Högskola, Sweden, in 2003, and the Ph.D. degree in Solid Mechanics from Luleå Tekniska Universitet, Sweden, in 2013. Since 2014 he is a lecturer with the Mechanical and Production Engineering Department, University of Mauritius, Mauritius. His research interests include solid mechanics, vibration and signal analysis, rotordynamics, signal processing, electromechanics and software development with the Ada programming language.